Revista Brasileira de Geofísica
RBGf
Brazilian Journal of Geophysics

Revista Brasileira de Geofísica (2006) 24(4): 547-557

ISSN 0102-261X
www.scielo.br/rbg

POLLUTANT TRANSPORT IN A CONVECTIVE BOUNDARY LAYER WITH LES

Edson Pereira Marques Filho[1], Amauri Pereira de Oliveira[2], Umberto Rizza[3] and Hugo Abi Karam[4]

Recebido em 23 agosto, 2006 / Aceito em 13 dezembro, 2006
Received on August 23, 2006 / Accepted on December 13, 2006

ABSTRACT. This work describes the statistical properties of a Convective Boundary Layer (CBL) and the associated turbulent transport of a passive and inert pollutant, continuously emitted in the atmosphere by an area-source on the surface. The CBL flow and properties are simulating with a Large Eddy Simulation (LES) model. To assure the development of a quasi-steady turbulent regime, both the stability parameter and the Turbulent Kinetic Energy (TKE) criteria were applied to LES with similar results. The vertical structure of the pollutant concentration, potential temperature associated with vertical turbulent fluxes and variances are consistent with the mixed layer similarity predictions. Both the pollutant concentration and the vertical wind skewness fluctuations are associated with the updrafts and downdrafts distributions, emphasizing the importance of the entrainment in the cleaning of the CBL.

Keywords: LES model, Convective Boundary Layer, Pollutant dispersion, Numerical models.

RESUMO. Este trabalho descreve as propriedades estatísticas de uma Camada Limite Convectiva (CLC) e o transporte turbulento de um poluente inerte e passivo, emitido continuamente por uma fonte do tipo área localizada na superfície. As propriedades da CLC são simuladas numericamente com o modelo de simulação direta dos grandes turbilhões (LES). A determinação da condição de quase-equilíbrio realizada com base no parâmetro de estabilidade para a CLC mostrou-se equivalente ao procedimento padrão, que utiliza os valores da energia cinética turbulenta integrada na camada. A estrutura vertical da concentração do poluente, temperatura potencial, e dos respectivos fluxos turbulentos e variâncias estão de acordo com os prognósticos da teoria da similaridade para a camada de mistura. Os parâmetros de assimetria da flutuação de concentração do poluente e da velocidade vertical refletem o padrão assimétrico das estruturas na CLC e indicam a importância dos processos de entranhamento na limpeza da camada.

Palavras-chave: Modelo LES, Camada Limite Convectiva, Dispersão de Poluentes, Modelagem Numérica.

[1]Department of Meteorology, Institute of Geosciences, Federal University of Rio de Janeiro, Av. Brigadeiro Trompowski, s/n, Bloco G, Ilha do Fundão, Cidade Universitária, 21941-590 Rio de Janeiro, RJ, Brasil. Tel.: (+55) 21 25989471; Fax: (+55) 21 25989474 – E-mail: emarques@acd.ufrj.br

[2]Department of Atmospheric Sciences, Institute of Astronomy, Geophysics and Atmospheric Sciences, University of São Paulo, Rua do Matão, 1226, 05508-900 São Paulo, SP, Brasil. – E-mail: apdolive@usp.br

[3]Istituto di Scienze dell'Atmosfera e del Clima (ISAC-CNR), Str. Prov. Lecce, Monteroni Km 1.200, Polo Scientifico dell'Università, 73100 Lecce, Itália. – E-mail: rizza@le.isac.cnr.it

[4]Department of Meteorology, Institute of Geosciences, Federal University of Rio de Janeiro, Av. Brigadeiro Trompowski, s/n, Bloco G, Ilha do Fundão, Cidade Universitária, 21941-590 Rio de Janeiro, RJ, Brasil – E-mail: hakaram@acd.ufrj.br

INTRODUCTION

The turbulent motions in Convective Boundary Layer (CBL) are dominated by eddies with length scale of the order of the Planetary Boundary Layer (PBL) height. In these conditions, the classical ensemble-mean closure models (K-approach, for example) present some deficiencies, mainly in the description of transport of pollutants carried out by the dominant eddies (Holtslag & Moeng, 1991). For convective conditions these turbulent eddies are able to transport pollutants and among other atmospheric properties against the gradient. Large Eddy Simulation (LES) model provides a valid alternative to estimate the turbulent transport in the CBL. They solve, directly, the motion generated by large eddies, describing accurately the turbulent transport of pollutants in the PBL.

Deardorff (1972) carried out the first LES application to simulate pollutant transport in the CBL. In his pioneer work, Deardorff established the scaling parameters of velocity and length, which, later on, revealed to be the most appropriate way to describe the vertical structure of the PBL statistical properties under convective conditions. Lamb (1984) has extensively applied the Deardorff's results for defining the PBL parameters for pollutant dispersion studies.

One of the first attempts to address the complexity of turbulent diffusion of a scalar in the CBL was done by Wyngaard & Brost (1984) and Moeng & Wyngaard (1984). Their results indicated that vertical gradients of concentration near to the top and bottom of CBL are driven by different physical processes. They found out that the vertical distribution of scalar turbulent flux is a superposition of top-down and bottom-up diffusion components driven, respectively, by fluxes at the top and bottom of the CBL. Some of these results were validated by Piper et al. (1995) utilizing a convection tank to simulate dispersion. Cuijpers & Holtslag (1998) proposed expressions for scalar and buoyancy vertical turbulent fluxes that combine local and nonlocal effects by using a generalized convective scaling. Sorbjan (1999) derived new expressions to describe the top-down processes that improved considerable the behavior of dimensionless gradients simulated by LES in the top of the CBL.

Nieuwstadt & Valk (1987) and van Haren & Nieuwstadt (1989) used a LES to simulate the patterns of air pollution dispersion in the CBL produced by continuously emitting point source using an instantaneous line source as surrogate. In this simulation, the plume generated by a pollutant released continuously from a source located at the surface rises up generating a maximum in concentration field at the top of PBL. In contrast, the pollutant released from sources located above the Surface Layer (SL) is transported down to the ground, causing a maximum concentration at the surface. These results are in agreement with classic convection tank experiment carried out by Willis & Deardorff (1976) and (1978). To reproduce this behavior became a standard procedure to validate LES capability to simulate dispersion of pollutants released continuously in a point source in a horizontally homogeneous convective PBL (Marques Filho, 2004).

The objective of this work is to describe the statistical properties of a highly convective PBL over a homogeneous surface simulated numerically by the LES developed by Moeng (1984). Here, a highly convective PBL is the one in which the stability parameter z_i/L is greater than -800. Special attention will be given to the characterization of turbulent transport of pollutant associated to continuously emitting area source located at the surface, under highly convective condition. This condition is commonly observed in subtropical areas of Brazil, like São Paulo State, during all seasons, and is related to calm wind and intense to moderate incoming solar radiation fluxes periods (Oliveira et al., 1998; 2002; 2003). These urban areas are very populated, and are emitting considerable amounts of pollutants, specially carbon monoxide (CO). For instance, the Metropolitan Area of São Paulo (8,051 km^2) emitted about 1,744,700 ton CO (CETESB, 2004). Approximately 98% of this emission is due to 7 million vehicles, and under low wind conditions a considerable fraction of this CO remains in the metropolitan area generating highly concentrations in intense traffic regions. To describe the behavior of pollutants under these conditions is important not only to improve the air quality management but also contribute to understand how this atmospheric contaminant is removed from the PBL.

In this work, the time evolution from the spatial structure of an atmospheric pollutant will be presented using the LES. In this simulation, the atmospheric pollutant is considered passive, conservative and continuously released by an area source located at the surface. The initial and boundary conditions were chosen to produce a well-defined free convection PBL.

Section two describes the theoretical formulations of the LES. The numerical scheme and initial and boundary conditions are presented in section three. Section four describes the criteria to identify the quasi-equilibrium turbulence and statistical properties of the PBL vertical structure. The conclusions are given in section five.

LES MODEL

The numerical simulation of the turbulent flows is carried out in LES solving directly the large eddies (resolved-scale). The small-scale part of the turbulent flow (subgrid-scale or SGS) is indirectly solved by parameterization techniques. This separation has been accomplished by a low-pass filtering applied in the prognostic variables (Leonard, 1974). The variables values, in the filtered equations of motion, are equivalent to volume-averaged values that describe only the resolved-scale of turbulent flow (Deardorff, 1972).

According to Moeng (1984), the equations that describe the time and space evolution of the wind velocity components in the resolved-scale can be written as:

$$\frac{\partial \overline{u}}{\partial t} = \overline{\overline{v}\overline{\zeta_z}} - \overline{\overline{w}\overline{\zeta_y}} + f\overline{v} - \frac{\partial P^*}{\partial x} - \frac{\partial \langle \overline{p} \rangle}{\partial x} - \frac{\partial \tau_{uu}}{\partial x} - \frac{\partial \tau_{uv}}{\partial y} - \frac{\partial \tau_{uw}}{\partial z} \tag{1}$$

$$\frac{\partial \overline{v}}{\partial t} = \overline{\overline{w}\overline{\zeta_x}} - \overline{\overline{u}\overline{\zeta_z}} + f\overline{u} - \frac{\partial P^*}{\partial y} - \frac{\partial \langle \overline{p} \rangle}{\partial y} - \frac{\partial \tau_{vu}}{\partial x} - \frac{\partial \tau_{vv}}{\partial y} - \frac{\partial \tau_{vw}}{\partial z} \tag{2}$$

$$\frac{\partial \overline{w}}{\partial t} = \overline{\overline{u}\overline{\zeta_y}} - \overline{\overline{v}\overline{\zeta_x}} + \frac{\overline{\theta}}{\theta_0} g - \frac{\partial P^*}{\partial z} - \frac{\partial \tau_{wu}}{\partial x} - \frac{\partial \tau_{wv}}{\partial y} - \frac{\partial \tau_{ww}}{\partial z} - \left\langle \frac{\partial \overline{w}^*}{\partial t} \right\rangle \tag{3}$$

where overbar denotes the resolved-scale; $\langle\ \rangle$ the horizontal average; u, v and w are the velocity components, θ is the potential temperature; f is the Coriolis parameter; ζ_x, ζ_y and ζ_z are the vorticity components in x, y and z, respectively; τ_{ij} are the modified SGS Reynolds stress; p is the hydrostatic atmospheric pressure; θ_0 is the reference potential temperature; and P^* is the modified pressure.

The horizontal mean pressure gradients $-\partial\langle\overline{p}\rangle/\partial x$ and $-\partial\langle\overline{p}\rangle/\partial y$, in Eqs. (1) and (2), respectively, are treated as an external forcing and prescribed in the model through the geostrophic wind. This implicates that resolved-scale flow is continuously accelerated in the horizontal direction towards a basic state in a geostrophic equilibrium. In Eq. (3), the horizontal average of the vertical acceleration is removed to assure that $\langle\overline{w}\rangle$ and $\langle\partial\overline{w}/\partial t\rangle$ will remain near to zero during the evolution of the PBL (Moeng, 1984).

The filtered equations for energy and pollutant concentration conservations in the resolved-scale are given by:

$$\frac{\partial \overline{\theta}}{\partial t} = -\overline{\overline{u}\frac{\partial \overline{\theta}}{\partial x}} - \overline{\overline{v}\frac{\partial \overline{\theta}}{\partial y}} - \overline{\overline{w}\frac{\partial \overline{\theta}}{\partial z}} - \frac{\partial \tau_{\theta u}}{\partial x} - \frac{\partial \tau_{\theta v}}{\partial y} - \frac{\partial \tau_{\theta w}}{\partial z} \tag{4}$$

$$\frac{\partial \overline{c}}{\partial t} = -\overline{\overline{u}\frac{\partial \overline{c}}{\partial x}} - \overline{\overline{v}\frac{\partial \overline{c}}{\partial y}} - \overline{\overline{w}\frac{\partial \overline{c}}{\partial z}} - \frac{\partial \tau_{cu}}{\partial x} - \frac{\partial \tau_{cv}}{\partial y} - \frac{\partial \tau_{cw}}{\partial z} \tag{5}$$

where c is the pollutant concentration (expressed as the mass of pollutant divided by the total air mass per unity of air volume in ppm), S_0 is the source term, $\tau_{\theta j}$ and τ_{cj} are SGS fluxes of sensible heat and pollutant.

The SGS terms in Eqs. (1)-(5) are related to the resolved-scale field through the eddy diffusivity coefficients. In this LES version, these coefficients are parameterized using the modified nonlinear eddy viscosity formulation proposed by Sullivan et al. (1994) and the Turbulent Kinetic Energy (TKE) in the subgrid-scale is estimated from the prognostic equation proposed by Deardorff (1980).

NUMERICAL SCHEME AND BOUNDARY CONDITIONS

This LES version developed by Moeng (1984) employs a pseudospectral method in the horizontal directions and a second-order centered in space finite-difference scheme in the vertical direction. The time derivatives are solved using Adams-Bashforth scheme. The lateral boundary conditions are periodic.

The turbulent fields are initialized by adding random fluctuations of wind velocity components, potential temperature and pollutant concentration to each respective initial profile. At the surface, the sensible heat is prescribed and the basic state potential temperature is evaluated as the mean potential temperature in the SL.

At the upper boundary, the vertical velocity, SGS turbulence fields and vertical gradients of horizontal velocity components are set equal to zero. The vertical gradient of potential temperature and pollutant concentration are kept constant.

The model was run for 2000 time steps, with 80 by 80 by 80 grid points in x, y and z, respectively, covering a numeric domain of 5 km by 5 km by 2 km. The numerical stability is verified every computational time step in agreement with the Courant-Friedrichs-Lewy (CFL) condition (Mesinger & Arakawa, 1976). In the simulation carried out here, the time step varied between 1.2 and 2.7 seconds, corresponding to a total time of about

1.5 hours of PBL time evolution. It required about 40 h of CPU time on a Cray J90.

The initial conditions for pollutant concentration and potential temperature correspond to a mixed layer with vertical extension of 1000 m. Their mixed layer values are given by the potential temperature (298K) and pollutant concentration (10 ppm) at the surface. The vertical profiles of horizontal velocity components (u, v) are assumed to be constant and equal to a zonal geostrophic wind of 1 ms^{-1}.

In agreement with the proposed values of Marques Filho (2004), the surface sensible heat flux was set 240 W m^{-2}, and the pollutant diffusion flux, 0.18 ppm m^{-2} s^{-1}, throughout the simulation. These conditions were defined to generate a PBL characterized by free convection regime.

RESULTS

The results presented hereafter are based on the three-dimensional fields generated after the first 1000 time steps (approximately 0.8 hours), when the CBL has reached a state of equilibrium (see section 4.1). The vertical profiles are ensemble average obtained of six outputs, separated by 200 time steps each.

The statistical moments and other relevant quantities were normalized using the mixed layer characteristic scales (Deardorff, 1972). The vertical coordinate was normalized by PBL height (z_i), defined as the height where the sensible heat flux reaches its minimum value. The second-order and third-order statistical moments were calculated considering the fluctuations of resolved-scale with respect to the horizontal-plane average $\left(u_i' = \overline{u_i} - \langle \overline{u_i} \rangle\right)$.

The mean turbulent parameters of simulated CBL considering those initial conditions are presented in Table 1:

Quasi-Steady Equilibrium

The turbulent flow in PBL reaches a quasi-steady equilibrium when its properties vary with a time scale smaller than the time scale of the boundary conditions and external forcing variations. In other words, the modifications existent in the boundaries and external forcing propagate fast enough along the PBL, adjusting them almost instantaneously to their time evolution. Under this condition, the PBL statistical properties can be determined as a function of the PBL characteristic scales, which in turn are defined as a function of the boundary conditions, external forcing and the intrinsic turbulent flow characteristics (Sorbjan, 1986).

In most of the LES applications, the quasi-steady equilibrium is determined by following the time evolution of TKE averaged over the entire PBL. The PBL is considered in equilibrium when its average TKE stops to oscillate (Nieuwstadt et al., 1992).

An equivalent and simpler way to identify the quasi-steady equilibrium during a LES simulation of a highly convective PBL is following the temporal evolution of the stability parameter $-z_i/L$. In Fig. (1a) the time evolution of $-z_i/L$ is shown during the period of simulation normalized by the characteristic time scale $0 < t/t_* \leq 8.1$ $(0h < t \leq 1.5h)$. It is possible to verify in this figure that after an initial overshoot $(t \leq 4.7t_*)$, $-z_i/L$ settles down around 880. This time period can be interpreted as the time after which the simulated CBL have reached the quasi-steady equilibrium. The overshoot is presumably caused by the initial development of large convective rolls, which turn into more random motions after the quasi-steady equilibrium (Nieuwstadt et al., 1992). It is possible to shown that the small, but visible (Fig. 1a), variation of $-z_i/L$ after $t = 4.7t_*$ is associated to incipient growth of the PBL height $(\partial z_i/\partial t > 0)$.

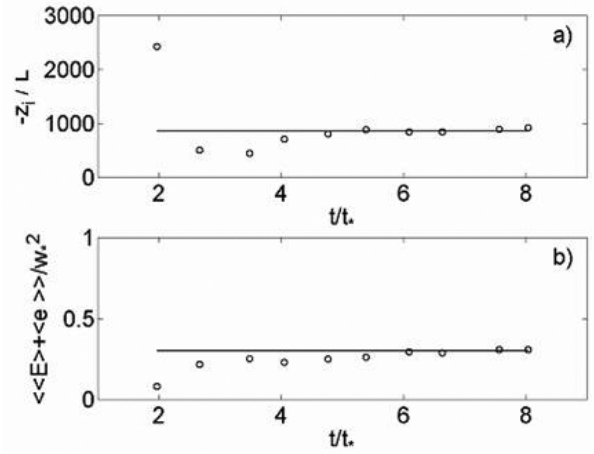

Figure 1 – Time evolution of: (a) stability parameter, and (b) turbulent kinetic energy. The horizontal lines correspond to $-z_i/L = 880$ and $\langle\langle \overline{E} \rangle + \langle e \rangle\rangle = 0.30w_*^2$.

The time evolution of TKE averaged over the entire PBL $\langle\langle \overline{E} \rangle + \langle e \rangle\rangle$ as a function of the dimensionless time t/t_* (Fig. 1b) indicates a similar behavior. After $t = 4.7t_*$, $\langle\langle \overline{E} \rangle + \langle e \rangle\rangle$ becomes approximately constant $(\approx 0.30w_*^2)$. Thus, the temporal evolution of $-z_i/L$ and $\langle\langle \overline{E} \rangle + \langle e \rangle\rangle$ are equivalent criteria indicating that the PBL turbulence simulated by LES reaches the quasi-steady equilibrium at about the same time.

The advantage of $-z_i/L$ criteria is that it is easier to implement numerically compared to the $\langle\langle \overline{E} \rangle + \langle e \rangle\rangle$ criteria. The case presented here can be set as a threshold condition to the $-z_i/L$ criteria, because this criterion does not work well when the thermal stability in the entrainment layer is weaker than the one used in this simulation. This restriction is not critical since most of

Table 1 – PBL characteristic scale values after 2000 time steps $(t \approx 1.5h)$.

$z_i(m)$	$-z_i/L$	$u_*(ms^{-1})$	$w_*(ms^{-1})$	$T_*(K)$	$c_*(ppm)$	$t_*(s)$
1475	882	0.174	2.246	0.107	0.080	656.65

the CBL simulations carried out with LES thermal stability of the entrainment layer is larger than one used here.

Turbulent and Mean Vertical Structures

The vertical profile of pollutant concentration $\langle\overline{c}\rangle$ indicates a decreasing in the mixed layer concentration values during the simulation associated to the large entrainment of clean air at the PBL top (Figs. 2a) (Wyngaard & Brost, 1984; Moeng & Wyngaard, 1984; Sorbjan, 1999). It will be showed later the entrainment is stronger for an intense convective PBL as the simulated.

The time scale for the pollutant be able to reach the PBL top was of order of $t_* \approx 657s$ (Table 1), and it implies an effective vertical mixing as expected for a highly convective PBL $(-z_i/L \approx 880)$. This value is smaller than the known time scale $t_* \approx 1096s$ obtained by Schmidt & Schumann (1989), but in agreement with the suggested by Sorbjan (1986).

In the vertical profile of potential temperature $\langle\overline{\theta}\rangle$ (Fig. 2b) is possible to observe the formation of a very extensive mixed layer $(\partial\langle\overline{\theta}\rangle/\partial z \approx 0)$. Near to the PBL top, the variations of $\langle\overline{\theta}\rangle$ are directly related to the free atmosphere lapse-rate. After reaching the quasi-steady equilibrium, the mixed layer is warmed about 0.5 K. This augment is consistent with the heating rate of 1.8×10^{-4} Ks^{-1}, estimated from

$$\frac{\partial\langle\overline{\theta}\rangle}{\partial t} = -\frac{\left[(\langle w'\theta'\rangle)_i - (\langle w'\theta'\rangle) + \tau_{\theta w}\right]_0}{z_i}$$

(Tennekes, 1973).

The vertical profile of mean horizontal wind, $\langle\overline{U}\rangle$, oscillate around the geostrophic wind value (Fig. 2c). Near the surface $z < 300$ m a logarithmic wind profile is observed. Above this, the vertical gradient of $\langle\overline{U}\rangle$ becomes approximately null, indicating the turbulence activity tends to homogenize the horizontal components of momentum in a barotropic CBL.

The dimensionless vertical turbulent pollutant fluxes

$$\frac{(\langle w'c'\rangle + \langle\tau_{cw}\rangle)}{w_* c_*}$$

vary linearly in the mixed layer (Fig. 3a), reaching a maximum at $z \approx 0.8z_i$ and decaying to zero above the inversion layer. The flux of pollutant in the CBL is divergent and $\partial\langle\overline{c}\rangle/\theta t < 0$, as observed in Fig. (2a).

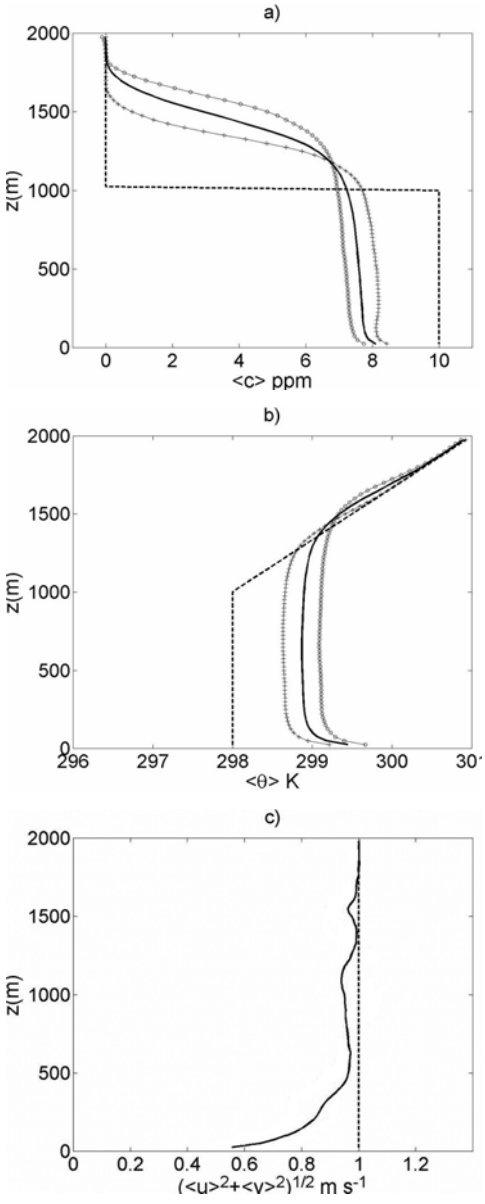

Figure 2 – Vertical profiles of: (a) pollutant concentration $\langle\overline{c}\rangle$, (b) potential temperature $\langle\overline{\theta}\rangle$, and (c) mean horizontal wind. The initial conditions are indicated by $(- - -)$, the vertical profiles at $t = 4.7t_*$ by $(- + -)$ and $t = 8.1t_*$ by $(- \circ -)$, and the ensemble averaged is indicated by $(-)$.

The pollutant flux due to entrainment processes can be related to the difference of pollutant concentration across the inversion layer $(\Delta\overline{c})$ and to the entrainment rate $(w_e = \partial z_i/\partial t)$ through the equation $(\langle w'c'\rangle + \langle\tau_{cw}\rangle)_i = -\langle\Delta\overline{c}\rangle w_e$ (Tennekes, 1973).

After the quasi-steady equilibrium the ensemble average yields $w_e = (0.09 \pm 0.02)$ ms^{-1} and $\langle \Delta \overline{c} \rangle = -(6.95 \pm 0.18)$ppm, resulting in $(\langle w'c' \rangle + \langle \tau_{cw} \rangle)_i = (0.63 \pm 0.14)$ ppm ms^{-1}. The value of $(\langle w'c' \rangle + \langle \tau_{cw} \rangle)_i$ obtained from averaging vertical flux at the PBL top is (0.53 ± 0.07) ppm ms^{-1}, agrees well with the value estimated using the mixed layer jump model.

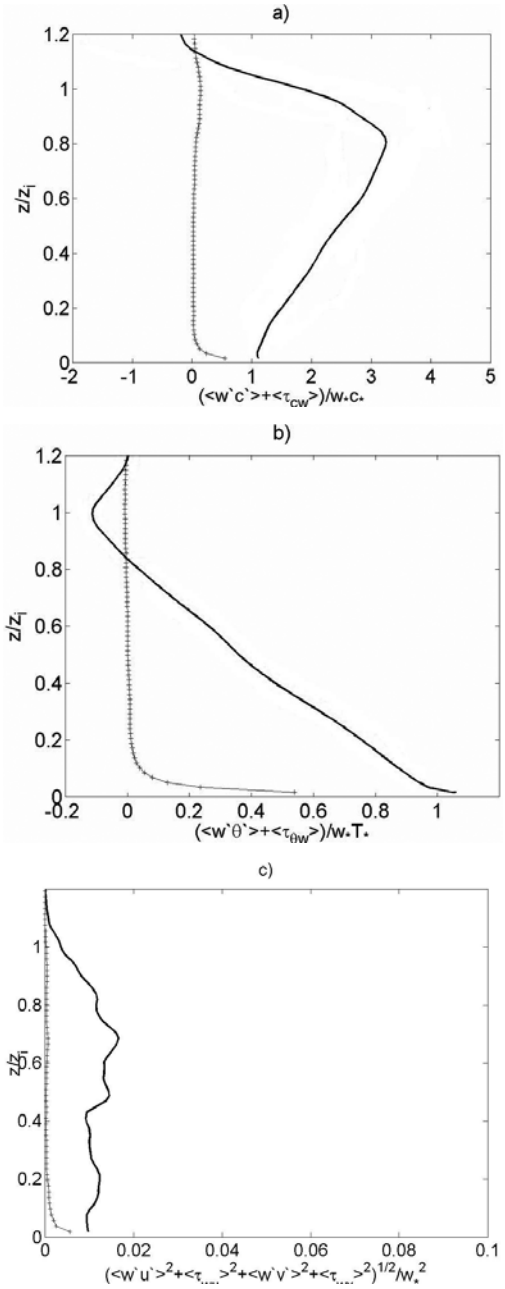

Figure 3 – Profiles of vertical turbulent flux of: (a) pollutant concentration, (b) sensible heat, and (c) total horizontal momentum. The ensemble average is indicated by $(--)$ for resolved plus subgrid scales and by $(- + -)$ for only subgrid scale.

The dimensionless vertical turbulent sensible heat flux

$$\frac{(\langle w'\theta' \rangle + (\langle \tau_{\theta w} \rangle)}{w_* T_*}$$

(Fig. 3b) shows also a linear variation with height in the mixed layer. This linear profile induces a constant heating rate in the mixed layer, as expected for CBL in equilibrium. Near to the PBL top, $(\langle w'\theta' \rangle + (\langle \tau_{\theta w} \rangle)$ reaches a minimum of $-(0.11 \pm 0.01) w_* T_*$, that is smaller than the value $-(0.17 \pm 0.02) w_* T_*$ suggested by Schmidt & Schumann (1989), but in agreement with the value $-0.11 w_* T_*$ after Moeng (1984) and $-0.12 w_* T_*$ by Nieuwstadt et al. (1992).

The SGS sensible heat flux $\langle \tau_{\theta w} \rangle$ contributes significantly to the total flux near the surface, decreasing drastically to zero above the height $0.2 z_i$.

The dimensionless vertical turbulent total momentum flux (Fig. 3c) is smaller compared with the vertical heat and pollutant fluxes because the TKE buoyancy production is the main forcing of the turbulence in a convective PBL.

Vertical Profile of Variances

The structure of the dimensionless vertical velocity variance $\langle w'^2 \rangle / w_*^2$, showed in Fig. (4a), reaches a maximum value of $(0.43 \pm 0.03) w_*^2$ at $z \approx 0,34 z_i$, in agreement with $0.44 w_*^2$ at $z \approx 0.33 z_i$ after Deardorff (1974). The $\langle w'^2 \rangle / w_*^2$ slowly decreases above this level, reaching a value of $(0.12 \pm 0.01) w_*^2$ at the PBL top.

Comparing the simulation carried out here with the fitted curve $\overline{[w'^2]} / w_*^2 = 1.8 (z/z_i)^{\frac{2}{3}} (1 - 0.8 z/z_i)^2$ (Lenschow et al., 1980), reveals that there is a good matching between them in the lower half of the PBL (Fig. 4a). There, the small difference is due to the fact that the SGS contribution was not included because it was not estimated directly in this simulation. In fact, $\langle \tau_{ww} \rangle$ was estimated assuming the isotropy hypothesis: $\langle \tau_{ww} \rangle = (2/3) \langle e^* \rangle$ (Nieuwstadt et al., 1992). Despite the discrepancies in the upper half of the CBL, the results obtained here are similar to Schmidt & Schumann (1989), who found that their results fitted better to the experimental data provided by Lenschow et al. (1980).

The dimensionless horizontal velocity component variances, $\langle u'^2 \rangle / w_*^2$ and $\langle v'^2 \rangle / w_*^2$, (Figs. 4b and 4c) are approximately constant and smaller than $\langle w'^2 \rangle / w_*^2$ in large portions of the mixed layer. This happens because in the CBL the TKE is generated mostly by the buoyancy production term, that contributes directly to the $\langle w'^2 \rangle$. Near the surface, the pressure fluctuation effects overcome the buoyancy effect (Schmidt & Schumann, 1989), and

$\langle u'^2, v'^2\rangle/w_*^2$ are larger than $\langle w'^2\rangle/w_*^2$. The SGS contributions of $\langle u'^2, v'^2\rangle/w_*^2$ are significantly smaller than the resolved-scale and also estimated using the isotropy hypothesis.

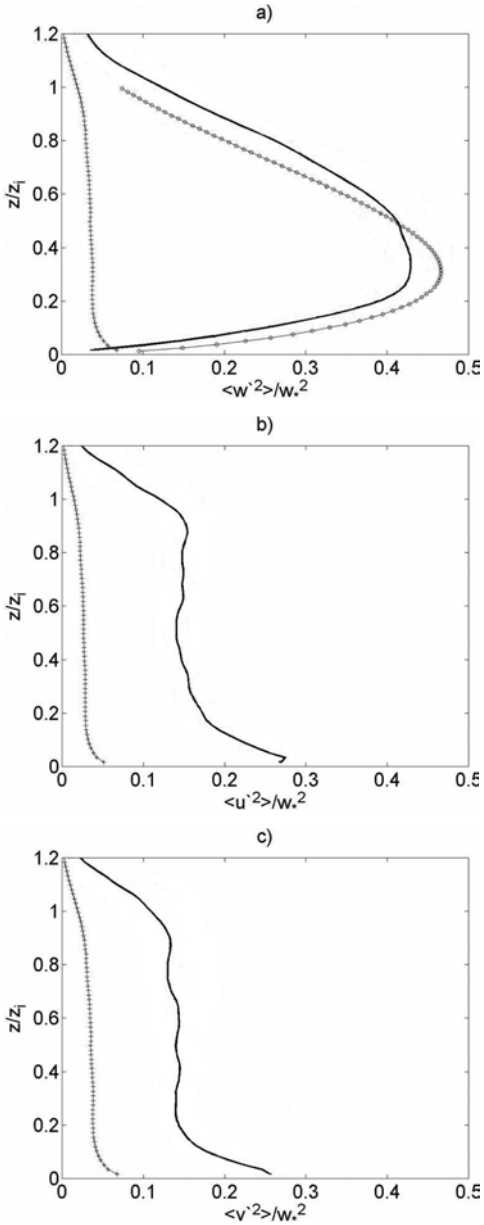

Figure 4 – Vertical profiles of variance for: (a) vertical, (b) zonal, and (c) meridional components of wind velocity. The empirical curve proposed by Lenschow et al. (1980) is indicated by $(-\circ-)$.

The variance of pollutant concentration $\langle c'^2\rangle/c_*^2$ is approximately constant until $z \approx 0.2z_i$ (Fig. 5a), because the vertical gradient of $\langle c\rangle$ in this region are not large enough (Fig. 2a). Above this level, it increases reaching a maximum near to the PBL top that is related to the large variation of $\langle\overline{c}\rangle$in the entrainment layer (Deardorff, 1974).

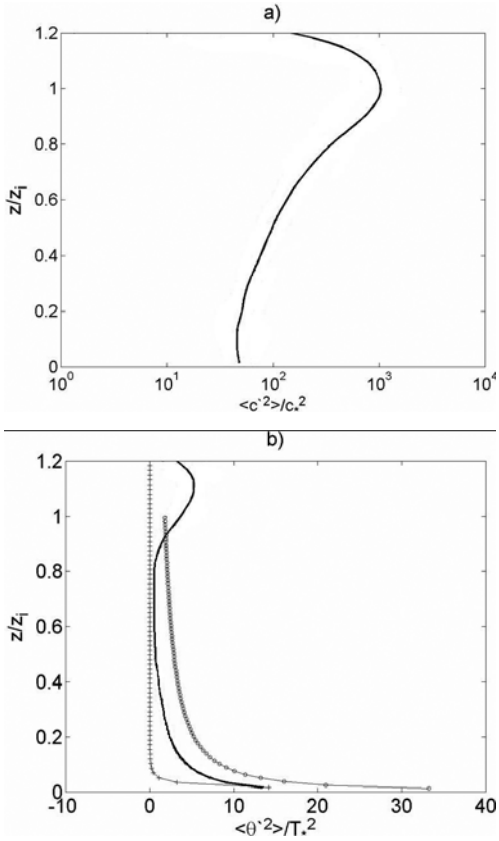

Figure 5 – Profiles of variance of: (a) pollutant concentration, and (b) potential temperature. The empirical curve proposed by Kaimal et al. (1976) is indicated by $(-\circ-)$.

The dimensionless potential temperature variance, $\langle\theta'^2\rangle/T_*^2$, presented in Fig. (5b), show a maximum at the surface, responding to the large vertical gradient of $\langle\theta\rangle$ (Fig. 2b). The $\langle\theta'^2\rangle/T_*^2$ profile drops with the height until the middle of the CBL, where it starts to increase, reaching a secondary maximum at the entrainment layer. The SGS variance of potential temperature is estimated according to $\langle\tau_{\theta\theta}\rangle = (0.67)^{-4}\langle\tau_{\theta w}\rangle^2/\langle e^*\rangle$ (Nieuwstadt et al., 1992).

In comparison to the experimental fitted curve proposed by Kaimal et al. (1976), $\overline{[\theta'^2]}/T_*^2 = 1.8(z/z_i)^{-2/3}$, the vertical profile of $\langle\theta'^2\rangle/T_*^2$ were underestimate. This difference is larger near the surface and is associated to the SGS contribution $\langle\tau_{\theta\theta}\rangle$. Besides, the fluctuations of potential temperature in the CBL are small and the instrumental errors become important enough to cast some doubts about the observations (Schmidt & Schumann, 1989).

Asymmetry

The CBL turbulence is characterized by asymmetric structures composed of updraft and downdraft. The updrafts are origina-

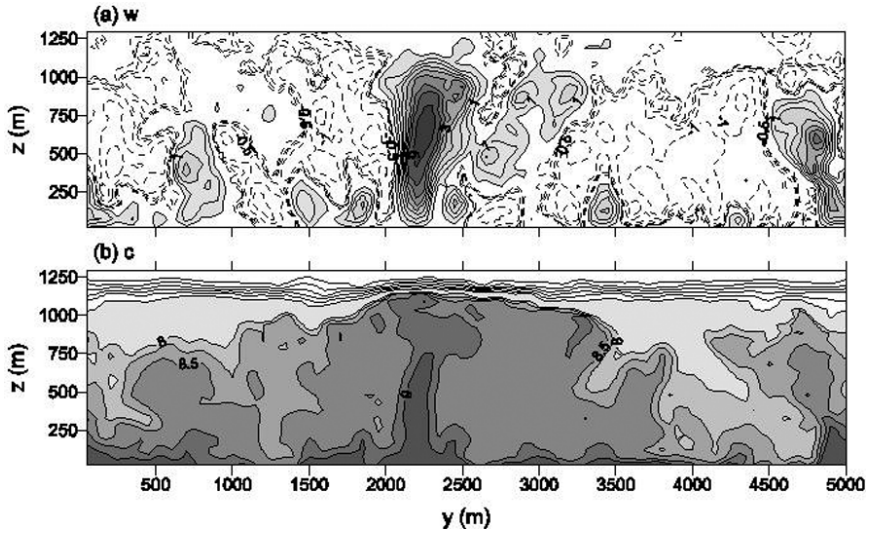

Figure 6 – Contour plots of: (a) vertical velocity component (ms^{-1}), and (b) pollutant concentration (ppm). In (a), the solid contours and the dark shaded area indicate positive vertical motions, and the dashed contours and the light shaded area negative motions. In (b), the dark shaded area indicates high pollutant concentration, and light shaded area the low concentration values.

ted in the surface and remain confined to narrow regions as they move up towards the top of the CBL. The downdrafts spread over broader regions of the CBL, which gradually descend down to the surface. The characteristic length scales associated to this structure are of the order of z_i (Kaimal et al., 1976; Lamb, 1984).

Figure 6a shows the instantaneous vertical velocity field where it is possible to identify a well defined updraft (dark shaded area between $y = 2000$ m and 2500 m). The extensive regions of weak vertical motion indicated by the dashed lines and light shaded areas are associated with downdrafts.

The updraft penetrate the inversion capping and to induce a negative vertical flow. The result is a net transport of clean air from the free atmosphere into the CBL. In Fig. 6b, some entrainment is perceived near to the top of CBL (750 m $\leq z \leq 1250$ m) and the other light shaded areas ($y \leq 500$ m and 3500 m $\leq y \leq 4800$ m). Moreover, areas of high pollutant concentration are well correlated with updrafts areas, showing the importance of these coherent structures in the pollutant transport.

The skewness of the pollutant concentration, defined by $\langle c'^3 \rangle / \langle c'^2 \rangle^{3/2}$, is negative for almost all mixed layer (Fig. 7a), with exception of the regions near to the surface and PBL top. These negative skewness fluctuations confirm the penetration of clean air into the CBL. Similar results for humidity were presented for Bernard-Trottolo et al. (2004).

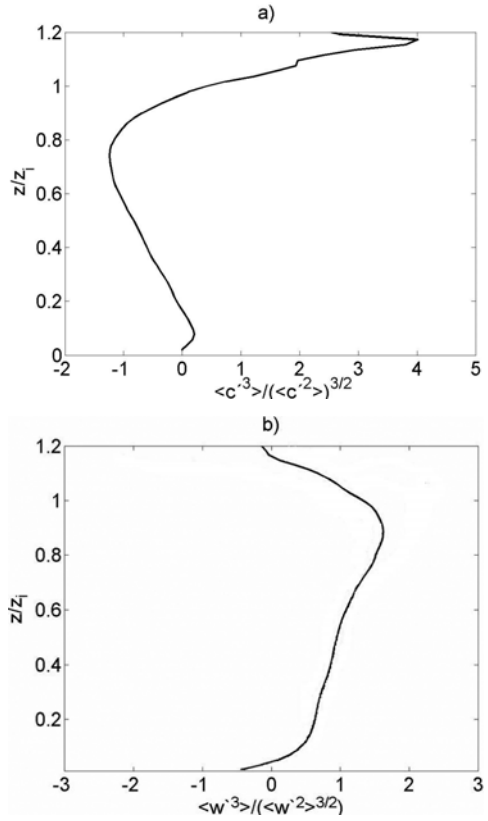

Figura 7 – Profiles of: (a) skewness of pollutant concentration, and (b) skewness of vertical wind velocity.

The analysis of the skewness of the vertical velocity $\langle w'^3\rangle/\langle w'^2\rangle^{3/2}$ also was evaluated (Fig. 7b), and indicates that the turbulence in the simulated CBL is positively asymmetric. This result confirms the presence of small and intensive updrafts and large and weak downdraft motions observed in the instantaneous field (Fig. 6a). The negative values near the surface are due to the inadequacy of the SGS model to handle free convection (Moeng, 1984; Schmidt & Schumann, 1989; Moeng & Rotunno, 1990). The values of $\langle w'^3\rangle/\langle w'^2\rangle^{3/2} \approx 0.44$ at $z \approx 0.1 z_i$, in agreement to the observations carried by Hunt et al. (1988) for convective PBL. Above $z \approx 0.1 z_i$, $\left\{\langle w'^3\rangle/\langle w'^2\rangle^{3/2}\right\}$ increases reaching a maximum of 1.62 at $z \approx 0.9 z_i$.

CONCLUSION

In this work, a LES is used to simulate a horizontally homogeneous CBL in order to describe the statistical properties of the PBL under low wind conditions. The turbulent transport of an inert and passive pollutant released continually by an area source located at the surface is analyzed as surrogate of CO dispersion under highly convective conditions, frequently observed in the city of São Paulo.

The LES version applied here is from Moeng (1984). The model was run for 2000 time steps, with 80 by 80 by 80 grid points in x, y and z, respectively, covering a numeric domain of 5 km by 5 km by 2 km. The time step varied between 1.2 and 2.7 seconds, corresponding to a total time of about 1.5 hours of PBL time evolution.

A new criterion based on the time evolution of $-z_i/L$ is proposed here in order to determine when the turbulence reaches its quasi-steady equilibrium, i.e., approximately 0.8 h. The result obtained following $-z_i/L$ can be considered equivalent to the method based on the TKE averaged over the entire PBL adopted by Nieuwstadt et al. (1992), because both implies similar quasi-steady equilibrium times.

The statistical analysis indicated that the LES was able to reproduce the main characteristics of a CBL under low wind shear $(-z_i/L \approx 880)$. Under this circumstance, the vertical profiles of the pollutant concentration, potential temperature and of mean horizontal wind followed the typical behavior observed in a well-mixed layer.

The vertical profiles of wind velocity variances followed the results available in the literature (Lenschow et al., 1980; Schmidt & Schumann, 1989). Even though the vertical profile of potential temperature and pollutant concentration variances presented a similar maximum at the top of CBL, the behavior of the pollutant did not follow the pattern obtained for the potential temperature (Kaimal et al., 1976).

Both the skewness of the pollutant concentration and vertical velocity are consistent with highly CBL (Moeng & Rotunno, 1990; Bernard-Trottolo et al., 2004). The strong correlation between space distribution of pollutant concentration and vertical velocity fluctuations confirms this asymmetric pattern (Deardorff, 1974; Schmidt & Schumann, 1989).

Even though the results obtained here were validated only for wind velocity components and potential temperature, they indicate that LES can be used to investigate the behavior of atmospheric pollutants for realistic conditions. A more definitive validation was not possible due to the lack of information about pollutant concentration in CBL.

ACKNOWLEDGEMENT

This research was supported by the Conselho Nacional de Desenvolvimento Científico e Tecnológico (Procs. CNPQ 140702/2000-8 and 300561/91-1) and by Fundação de Amparo à Pesquisa do Estado de São Paulo (Proc. FAPESP 98/15402-5). The authors thank the Laboratório de Computação Científica e Aplicada da Universidade de São Paulo for the computational support. We are also indebted to Dr. J. Soares for her suggestions during this research.

REFERENCES

BERNARD-TROTTOLO S, CAMPISTRON B, DRUILHET A, LOHOU F & SAÏD F. 2004. Trac98: detection of coherent structures in a convective boundary layer using airborne measurements. Boundary-Layer Meteorology, 111: 181–224.

CETESB. Companhia de Tecnologia de Saneamento Ambiental. 2004. Operação inverno 2003: Qualidade do ar. Relatório técnico, 101 pp. Disponível em: <http://www.cetesb.sp.gov.br/Ar/relatorios.asp>. Acesso em: 10 maio 2004.

CUIJPERS JWM & HOLTSLAG AAM. 1998. Impact of skewness and nonlocal effects on scalar and buoyancy fluxes in convective boundary layer. Journal of the Atmospheric Sciences, 55: 151–162.

DEARDORFF JW. 1972. Numerical investigation of neutral and unstable planetary boundary layers. Journal of the Atmospheric Sciences, 29: 91–115.

DEARDORFF JW. 1974. Three-dimensional numerical study of turbulence in an entraining mixed layer. Boundary Layer Meteorology, 7: 199–226.

DEARDORFF JW. 1980. Stratocumulus-capped mixed layers derived from a three-dimensional model. Boundary Layer Meteorology, 18: 495–527.

HOLTSLAG AAM & MOENG C.-H. 1991. Eddy diffusivity and countergradient transport in the convective atmospheric boundary layer. Journal of the Atmospheric Sciences, 48: 1690–1698.

HUNT JCR, KAIMAL JC & GAYNOR JE. 1988. Eddy structure in the convective boundary layer – new measurements and new concepts. Quart. J. Royal Meteorological Society, 114: 827–858.

KAIMAL JC, WYNGAARD JC, HAUGEN DA, COTÉ OR, IZUMI Y, CAUGUEY SJ & READINGS CJ. 1976. Turbulence structure in the convective boundary layer. Journal of the Atmospheric Sciences, 33: 2152–2169.

LAMB RG. 1984. Diffusion in the convective boundary layer. In: NIEUWSTADT FTM & VAN DOP H (Ed.). Atmospheric Turbulence and Air Pollution Modelling. D Reidel, Dordrecht, 159–229.

LENSCHOW DH, WYNGAARD JC & PENNEL WT. 1980. Mean-field and second-moment budgets in a baroclinic, convective boundary layer. Journal of the Atmospheric Sciences, 37: 1313–1326.

LEONARD A. 1974. Energy cascade in large-eddy simulations of turbulent fluid flows. Advances in Geophysics, 18: 237–248.

MARQUES FILHO EP. 2004. Investigação da Camada Limite Planetária Convectiva com Modelo LES Aplicado à Dispersão de Poluentes. Doctorate Thesis, University of São Paulo, São Paulo, SP, Brazil, 128 pp. Disponível em: <http://www.teses.usp.br>. Acesso em: 20 jul. 2006.

MESINGER F & ARAKAWA A. 1976. Numerical methods used in atmospheric models. Global Atmospheric Research Programme, WMO, 100 pp.

MOENG C.-H. 1984. A large-eddy simulation model for the study of planetary boundary-layer turbulence. Journal of the Atmospheric Sciences, 41: 2052–2062.

MOENG C.-H & WYNGAARD JC. 1984. Statistics of conservative scalars in the convective boundary layer. Journal of the Atmospheric Sciences, 41: 3161–3169.

MOENG C.-H & ROTUNNO R. 1990. Vertical-velocity skewness in the buoyancy-driven boundary layer. Journal of the Atmospheric Sciences, 47: 1149–1162.

NIEUWSTADT FTM & VALK JPJMM. 1987. A large eddy simulation of buoyant and non-buoyant plume dispersion in the atmospheric boundary layer. Atmospheric Environment, 21: 2573–2587.

NIEUWSTADT FTM, MASON PJ, MOENG C.-H & SCHUMANN U. 1992. Large-eddy simulation of the convective boundary layer: A comparison of four computer codes. In: DURST F, FRIEDRICH R, LAUNDER BE, SCHMIDT FW, SCHUMANN U & WHITELAW JH (Ed.). Turbulent Shear Flows 8. Springer, Berlin, 343–367.

OLIVEIRA AP, SOARES J, TIRABASSI T & RIZZA U. 1998. A surface energy-budget model coupled with a Skewed Puff Model for Investigating the Dispersion of radionuclides in a Subtropical area of Brazil. Il Nuovo Cimento, 21C: 631–637.

OLIVEIRA AP, ESCOBEDO JF, MACHADO AJ & SOARES J. 2002. Diurnal evolution of solar radiation at the surface in the City of São Paulo: seasonal variation and modeling. Theoretical and Applied Climatology, 71: 231–249.

OLIVEIRA AP, BORNSTEIN R & SOARES J. 2003. Annual and diurnal wind patterns in the city of São Paulo, Water, Air and Soil Pollution. FOCUS, 3: 3–15.

PIPER M, WYNGAARD JC, SNYDER WH & LAWSON JRE. 1995. Top-down, bottom-up diffusion experiments in a water convection tank. Journal of the Atmospheric Sciences, 52: 3607–3619.

SCHMIDT H & SCHUMANN U. 1989. Coherent structure of the convective boundary layer derived from large-eddy simulations. Journal Fluid Mechanics, 200: 511–562.

SORBJAN Z. 1986. On similarity in the atmospheric boundary layer. Boundary-Layer Meteorology, 35: 377–397.

SORBJAN Z. 1999. Similarity of scalar fields in the convective boundary layer. Journal of the Atmospheric Sciences, 56: 2212–2221.

SULLIVAN P, MCWILLIAMS JC & MOENG C.-H. 1994. A subgrid-scale model for large-eddy simulation of planetary boundary-layer flows. Boundary-Layer Meteorology, 71: 247–276.

TENNEKES H. 1973. A model for the dynamics of the inversion above a convective boundary layer. Journal of the Atmospheric Sciences, 30: 558–567.

VAN HAREN LV & NIEUWSTADT FTM. 1989. The behavior of passive and buoyant plumes in a convective boundary layer, as simulated with a large-eddy model. Journal Applied Meteorology, 28: 818–832.

WILLIS GE & DEARDORFF JW. 1976. A laboratory model of diffusion into the convective planetary boundary layer. Quart. J.R. Meteorological Society, 102: 427–445.

WILLIS GE & DEARDORFF JW. 1978. A laboratory study of dispersion from an elevated source in a convective mixed layer. Atmospheric Environment, 12: 1305–1313.

WYNGAARD JC & BROST RA. 1984. Top-down and bottom-up diffusion of a scalar in the convective boundary layer. Journal of the Atmospheric Sciences, 41: 102–112.

NOTES ABOUT THE AUTHORS

Edson Pereira Marques Filho. Professor of Meteorology at the Federal University of Rio de Janeiro since 2006. PhD in Meteorology at the Institute of Astronomy, Geophysics and Atmospheric Sciences of the University of São Paulo (2004). Published 5 articles in specialized journals and 1 book chapter. Areas of interest: Micrometeorology, Atmosphere-Surface Interactions.

Amauri Pereira de Oliveira. Professor of Meteorology at the Institute of Astronomy, Geophysics and Atmospheric Sciences of the University of São Paulo since 1994. PhD in Meteorology at the State University of New York in Albany-USA (1990). Published 25 articles in specialized journals and 1 book chapter. Areas of interest: Micrometeorology, Ocean-Atmosphere Interactions.

Umberto Rizza. Senior Researcher at the Institute of Atmospheric Sciences and Climate – Consiglio Nazionale delle Ricerche d'Italy – since 1994. Graduated in Physics at the University of Bologna (1989). Published 35 articles in specialized journals and 12 books chapters. Areas of interest: Micrometeorology, Dispersion Numerical Models.

Hugo Abi Karam. Professor of Meteorology at the Federal University of Rio de Janeiro since 2006. PhD in Meteorology at the Institute of Astronomy, Geophysics and Atmospheric Sciences of the University of São Paulo (2002). Published 5 articles in specialized journals. Areas of interest: Micrometeorology, Atmosphere-Surface Interactions.